High resolution-high energy x-ray photoelectron spectroscopy using third-generation synchrotron radiation source, and its application to Si-high *k* insulator systems

K. Kobayashi[a)] and M. Yabashi
JASRI/SPring-8, Kouto 1-1-1, Mikaduki-cho, Sayo-gun, Hyogo 679-5198, Japan

Y. Takata, T. Tokushima, and S. Shin
Soft X-Ray Spectroscopy Laboratory, RIKEN/SPring-8, Kouto 1-1-1, Mikaduki-cho, Sayo-gun, Hyogo 679-5148, Japan

K. Tamasaku, D. Miwa, and T. Ishikawa
Coherent X-Ray Optics Laboratory, RIKEN/SPring-8, Kouto 1-1-1, Mikaduki-cho, Sayo-gun, Hyogo 679-5148, Japan

H. Nohira and T. Hattori
Department of Electrical and Electronic Engineering, Musashi Institute of Technology, Tamazutsumi 1-28-1, Setagaya-ku, Tokyo 158-8557, Japan

Y. Sugita
Fujitsu Laboratories Ltd., Morinosato-Wakamiya, Atsugi 243-0197, Japan

O. Nakatsuka, A. Sakai, and S. Zaima
Graduate School of Engineering, Nagoya University, Furo-cho, Chikusa-ku, Nagoya 464-8603, Japan

High-resolution x-ray photoelectron spectroscopy (XPS) at 6 keV photon energy has been realized utilizing high-flux-density x rays from the third generation high-energy synchrotron radiation facility, SPring-8. The method has been applied to analysis of high-*k* HfO_2/interlayer/Si complementary metal–oxide–semiconductor gate-dielectric structures. With the high energy resolution and high throughput of our system, chemical-state differences were observed in the Si 1*s*, Hf 3*d*, and O 1*s* peaks for as-deposited and annealed samples. The results revealed that a SiO_xN_y interlayer is more effective in controlling the interface structure than SiO_2. Our results show the wide applicability of high resolution XPS with hard x rays from a synchrotron source. © *2003 American Institute of Physics.* [DOI: 10.1063/1.1595714]

Nondestructive chemical state analysis of layered materials is becoming more important for the current and future technologies of nanoscience and engineering. X-ray photoelectron spectroscopy (XPS), often referred as electron spectroscopy for chemical analysis, is widely used for this purpose. Various laboratory XPS instruments, which typically use Al $K\alpha$ (1486.6 eV) or Mg $K\alpha$ (1253.6 eV) lines for excitation, have become commercially available, serving as essential tools in device industries. The probing depth, which is material dependent, is limited at most to 4 nm for these energies due to strong inelastic scattering of photoelectrons.[1] Even excitation by strong soft x rays from synchrotron radiation cannot change the probing depth. Extension of the probing depth up to, say, 10 nm will greatly widen the applicability to various materials with nanolayered structures and nanoparticles.

A straightforward way to extend the probing depth is to raise the photon energy for excitation. What has prevented us from trying hard x-ray excitation is the rapid decrease in subshell photoionization cross sections with increasing excitation energy. Most elements have $10^{-2}–10^{-6}$ Mb photoionization cross sections of subshells at 8047 eV (Cu $K\alpha$), being two orders of magnitude smaller than those at 1486 eV (Al $K\alpha$).[2] Another problem is the decrease in transmissivity of the lens system in an electron analyzer with increasing electron kinetic energy. However, recent progress of x-ray undulators at third-generation synchrotron light sources enables delivery of unprecedented high photon flux as well as high flux density.[3,4] These sources can well compensate the decreases in cross section and analyzer transmission, and make high-energy and high-resolution XPS accessible.

The larger escape depth of photoelectrons with higher kinetic energy will facilitate studies of electronic structures and/or chemical states of bulk materials, nanoscale buried layers and their interfaces since the contribution to the detection of signal from the surface region will be small. Elaborate surface cleaning procedures, which have been established only for a limited number of materials, and UHV conditions for conventional XPS measurements will be unnecessary. This enables us both to make measurements with high turn-around and to measure materials so far inaccessible due to the lack of proper surface preparation methods. The probing depth for photon energies between 5 and 10 keV is estimated to range from around 5 to over 10 nm,[1] matching the characteristic thickness of layers used in various nanoscale devices of current technical interest.[5]

Experiments were performed at the undulator beam line,

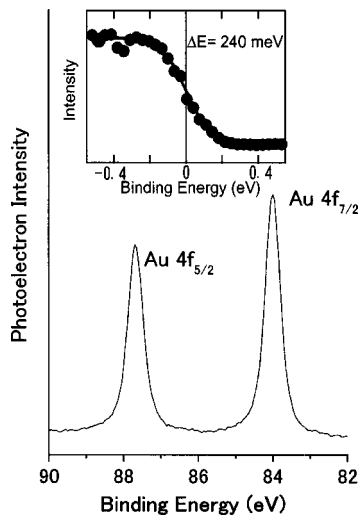[a)]Electronic mail: koba_kei@spring8.or.jp

FIG. 1. Au $4f$ core level spectra of a Au plate measured at 5950 eV excitation with $E_p = 200$ eV. The inset shows the Fermi edge spectra at 20 K with $E_p = 200$ eV. The total energy resolution was estimated as 240 meV for $E_p = 200$ eV from the Fermi edge broadening.

FIG. 2. Si $1s$ spectra measured for as-deposited and annealed (dotted) $HfO_2/SiO_2/Si(100)$ are compared with that measured for 1.32 nm $SiO_2/Si(100)$. The pass energy E_p is 200 eV. These spectra are normalized to the substrate peak.

BL29XU,[6] of SPring-8. X-rays monochromatized at 5950 eV, with a Si 111 double-crystal monochromator, were vertically focused with a cylindrically bent mirror onto samples mounted in an analyzer chamber. A channel-cut monochromator with Si 333 reflection placed downstream from the mirror reduced the energy bandwidth to 70 meV. At the sample position, the photon flux in a focal spot of 0.12 mm (vertical)$\times$0.7 mm (horizontal) was measured by a calibrated ionization chamber to be 2×10^{11} counts/s. The vacuum of the analyzer chamber was 10^{-4}–10^{-5} Pa during the measurements. A Gammadata Scienta SES2002, modified to accommodate higher photoelectron kinetic energies up to 6 keV, was used as an electron analyzer.

The performance of the detection system was tested by measuring Au $4f$ spectra with an analyzer pass energy (E_p) of 200 eV and a photoelectron take-off angle (measured from the sample surface) $\theta = 70°$. To confirm surface insensitivity, no surface treatment was made on the Au sample plate before or after introducing it into the analyzer chamber. Figure 1 shows observed spectra with accumulation times of 10 min at 80 mA ring current. The full width at half maximum of the Au $4f_{7/2}$ peak is 470 meV. Even with the high-energy excitation, the Fermi-edge of Au is clearly observed at 20 K as shown in the inset of Fig. 1. The instrumental energy resolution including the x-ray bandwidth is determined as 240 meV from the Fermi-edge profile. Comparable resolutions to that obtained here are also realized by laboratory XPS systems with a monochromator[7] only at the sacrifice of the throughput by c.a. one order of magnitude. Both the Au $4f$ and Fermi-edge spectra show no trace of surface contamination despite the absence of prior treatment of the sample.

The performance verified earlier tempted us to apply this method to analysis of high-k complementary metal–oxide–semiconductor (CMOS) gate dielectrics, which urgently need investigation for future Si-ultralarge scale integration (ULSI) devices.[8] Among various high-k dielectrics with a typical needed thickness of around 5 nm, HfO_2 is considered to be one of the most promising materials.[9] We prepared 4-nm-thick HfO_2 layers by atomic layer deposition (ALD) on 1 nm
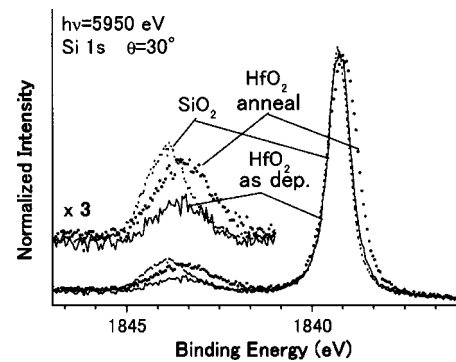
chemical oxide (SiO_2) layers.[10] Figure 2 shows Si $1s$ spectra of this $HfO_2/SiO_2/Si(100)$ structure with $\theta = 30°$ and $E_p = 200$ eV. The Si $1s$ spectra of a sample with 1.32 nm SiO_2 on Si(100) are shown as a reference. The acquisition time for each spectrum was approximately 10 min. The spectra are normalized to the substrate peaks. After deposition of the HfO_2 film, the Si $1s$ peak for the intermediate layer occurred at about 0.6 eV lower in binding energy and was broader than for the SiO_2 peak. This peak is attributed to Hf silicate, so that formation of Hf silicate has already taken place during the HfO_2 ALD. Annealing the sample at 1000 °C in dry nitrogen gas for 5 s enhanced the intensity of the Hf silicate peak. This result suggests that silicate formation is related to diffusion of Si atoms into the deposited layers from the Si substrate. A detectable increase in the spectral intensity appearing on the low binding-energy side of the substrate peak (as shown by the dotted curve in Fig. 2) indicates the formation of Hf–Si bonds by the annealing.

The changes in $HfO_2/SiO_2/Si$ and $HfO_2/SiO_xN_y/Si$ induced by annealing are more clearly examined from chemical shift in the Si $1s$, O $1s$ and Hf $3d$ spectra shown in Fig. 3. Chemically shifted Si $1s$ spectra can be decomposed into two components separated by 0.74 eV. The as-deposited $HfO_2/SiO_2/Si$ shows only the component with higher binding energy, while the annealed $HfO_2/SiO_2/Si$ shows both
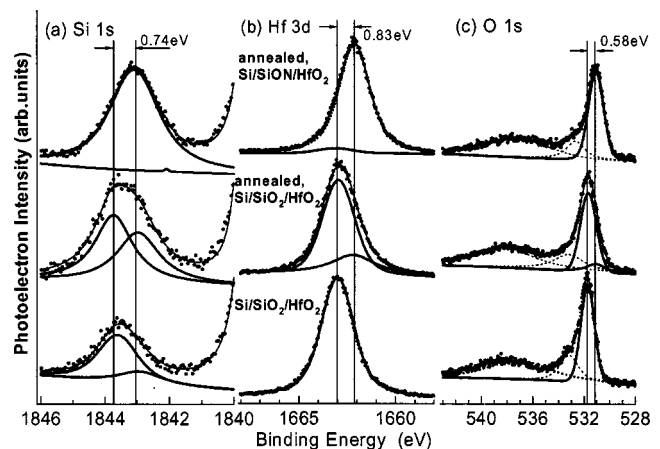

FIG. 3. Si $1s$, O $1s$, and Hf $3d$ spectra measured for as-deposited $HfO_2/SiO_2/Si$, annealed $HfO_2/SiO_2/Si$ and annealed $HfO_2/SiO_xN_y/Si$ with $E_p = 200$ eV. Dots show raw data, while smooth curves (thick, thin, and broken curves) indicate results of curve fits using Voigt functions.
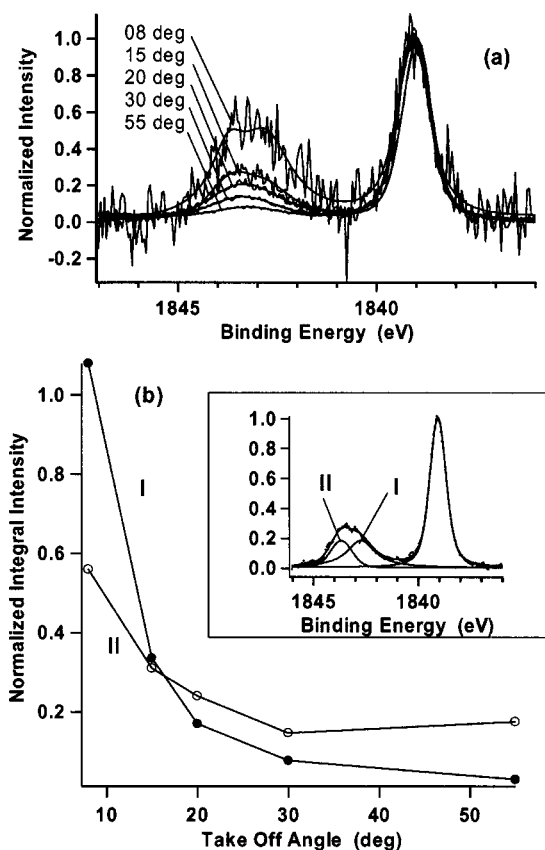
FIG. 4. (a) Si 1s spectra of annealed HfO_2/SiO_2/Si for various take-off angles. The smooth curves indicate curve fits using Voigt functions. (b) The chemical shifted Si 1s peaks were decomposed into two peaks (I and II) as shown in the inset. The integral intensity of each component is shown as a function of the take-off angle.

components. Annealed HfO_2/SiO_xN_y/Si shows only the component with lower binding energy. The position of the main O 1s and Hf 3d peaks for annealed HfO_2/SiO_xN_y/Si shift to lower energy by 0.58 and 0.83 eV, respectively, compared to those for annealed HfO_2/SiO_2/Si. The width of the Si 1s peak arising from the Si substrate for annealed HfO_2/SiO_xN_y/Si is 0.85 eV (not shown), and is narrower than the 0.98 eV width for annealed HfO_2/SiO_2/Si and wider than the 0.72 eV width for as-deposited HfO_2/SiO_2/Si, indicating less Si–Hf bond formation in the annealed SiO_xN_y interlayer sample than for the SiO_2 interlayer sample.

The two components appearing in the chemically shifted Si 1s peak for the annealed HfO_2/SiO_2/Si sample in Fig. 3 raise a question about the depth distribution of the components. To clarify this problem, the dependence of the Si 1s spectra on take-off angle, θ, was measured as shown in Fig. 4. The spectra for various θ were normalized to the Si substrate peak. The θ dependence of the integrated intensities for the two components is plotted in Fig. 4(b), and explicitly demonstrates that the lower binding-energy component is dominant at lower θ, while the higher binding-energy component dominates at higher θ. We deduce from this result that annealing leads to the formation of a two-layer structure. The

low binding-energy component comes from the layer near the surface while the higher binding-energy component comes from the layer near the substrate. The present results are inconsistent with the recent report of Lysaght *et al.*, who propose a four-layer model for an ALD-prepared HfO_2/SiO_2/Si structure annealed at 900 °C from secondary ion mass spectroscopy and medium-energy ion spectroscopy results.[11]

Together with the Hf–Si bond formation seen in Fig. 2, our present results indicate that 1 nm SiO_2 interlayer is not sufficient to block the interface reaction and that the HfO_2/SiO_2/Si structure is unstable against the annealing process. Recalling that annealing results in the formation of a single-phase Hf silicate and lesser Hf–Si bond formation in the HfO_2/SiO_xN_y/Si sample, we conclude that SiO_xN_y is more effective in preventing the interface reaction than SiO_2. It is to be noted that, even at a low θ of 8°, the substrate Si 1s peak is clearly detected in Fig. 4. Considering the 5 nm total thickness of the overlayer (1 nm SiO_2 + 4 nm HfO_2), we believe that we can prove buried layers as deep as 35 nm.

In summary, high-resolution XPS at 6 keV photon energy has been realized utilizing high-flux-density x rays from the third-generation high-energy synchrotron radiation facility, SPring-8. The method has been applied to high-k HfO_2/interlayer/Si CMOS gate-dielectric structures. Chemical-state differences observed in Si 1s, Hf 3d, and O 1s peak for as-deposited and annealed samples revealed that two phases of Hf silicates and Hf–Si bonding are formed during 5 s annealing at 1000 °C. In the annealed HfO_2/SiO_2/Si sample, measurement of Si 1s spectra as a function of take-off angle has shown that each Hf silicate phase has a different depth profile. These results indicate that SiO_xN_y as an interlayer is more effective in controlling the interface structure than SiO_2. Our present results show the wide applicability of high-resolution XPS using hard x rays from a synchrotron source.

[1] The electron inelastic-mean-free-paths were estimated using NIST Standard Reference Database 71, ''NIST Electron Inelastic-Mean-Free-Path Database: Ver. 1.1.'' It is distributed via the Web site http://www.nist.gov/srd/nist71.htm, and references therein.
[2] J.-J. Yeh and I. Lindau, At. Data Nucl. Data Tables **32**, 1 (1985).
[3] H. Kitamura, Rev. Sci. Instrum. **66**, 2007 (1995).
[4] H. Kitamura, J. Synchrotron Radiat. **7**, 121 (2000).
[5] These devices include ULSIs, magnetic memory devices, organic electroluminescent devices, and spin electronic devices.
[6] K. Tamasaku, Y. Tanaka, M. Yabashi, H. Yamazaki, N. Kawamura, M. Suzuki, and T. Ishikawa, Nucl. Instrum. Methods Phys. Res. A **467/468**, 686 (2001).
[7] U. Gelius, B. Wannberg, P. Baltzer, H. Fellner-Feldegg, G. Carlsson, C. G. Johansson, J. Larsson, P. Munger, and G. Vergerfos, J. Electron Spectrosc. Relat. Phenom. **52**, 747 (1990).
[8] International Technology Roadmap for Semiconductors, 2002 ed. Available from the International Technology Roadmap for Semiconductors web site, http://public.itrs.net/
[9] G. D. Wilk, R. M. Wallace, and J. M. Anthony, J. Appl. Phys. **89**, 5243 (2001).
[10] Y. Morisaki, Y. Sugita, K. Irino, and T. Aoyama, Ext. Abstr. Int. Workshop on Gate Insulator, Tokyo, 2001, p. 184.
[11] P. S. Lysaght, P. J. Chen, R. Bergmann, T. Messina, R. W. Murto, and H. R. Huff, J. Non-Cryst. Solids **303**, 54 (2002).